

Decoupling Geometrical and Chemical Cues Directing Epidermal Stem Cell Fate on Polymer Brush-Based Cell Micro-Patterns

Supporting Information

*Khooi Y. Tan¹, Hui Lin², Madeleine Ramstedt³, Fiona M. Watt⁴, Wilhelm T. S. Huck^{1,5} and
Julien E. Gautrot^{2*}*

¹ Melville Laboratory for Polymer Synthesis, Department of Chemistry, University of Cambridge,
Lensfield Road, Cambridge, CB2 1EW, UK.

² School of Engineering and Materials Science, Queen Mary, University of London, Mile End Road,
London, E1 4NS, UK.

³ Department of Chemistry, Umeå University, SE-90187 Umeå, Sweden.

⁴ Centre for Stem Cells and Regenerative Medicine, King's College London, Guy's Hospital, Great
Maze Pond, London, SE1 9RT, UK.

⁵ Radboud University Nijmegen, Institute for Molecules and Materials, Heyendaalseweg 135, 6525 AJ
Nijmegen, The Netherlands.

* To whom correspondence should be addressed E-mail: j.gautrot@qmul.ac.uk.

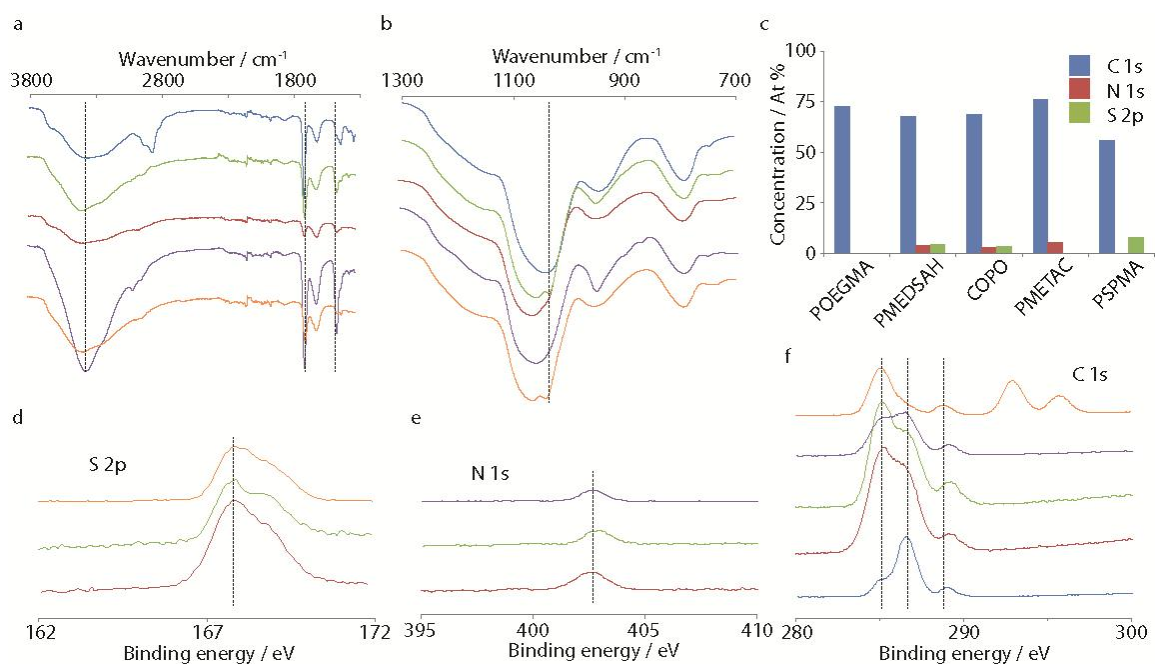


Figure S1. FTIR and XPS characterisation of polymer brushes. POEGMA, light blue; PMEDSAH, green; COPO, red; PMETAC, dark blue; PSPMA, orange. a, FTIR spectra of brushes in the 1300-3800 cm^{-1} and b, 700-1300 cm^{-1} range. The spectra were split because of the difference in intensity over the full range probed. c, Atom % from XPS measurements. d, S 2p, e, N 1s and f, C 1s XPS spectra. Only C, N and S are presented for clarity. The additional peaks in the C 1s part of the XPS spectrum of PSPMA arise from K.

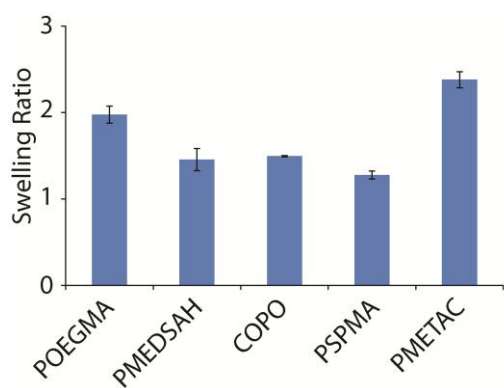


Figure S2. Swelling of polymer brushes. Swelling of polymer brushes upon immersion in PBS, measured by spectroscopic ellipsometry.

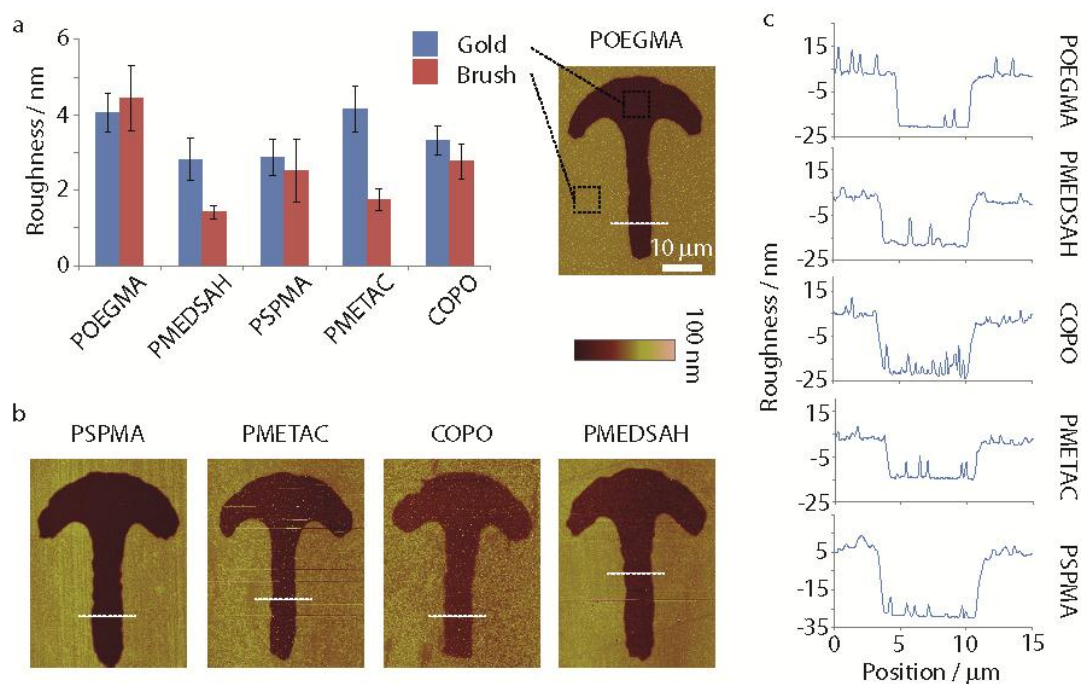


Figure S3. Topography of polymer brush-based micro-patterns. Arc-shaped micro-patterns were analysed via AFM in tapping mode (dry samples were analysed). a, Surface roughness inside and outside the patterns (dotted boxes) were measured (top left). b, Examples of single patterns are presented for each brush. c, Associated AFM height profiles.

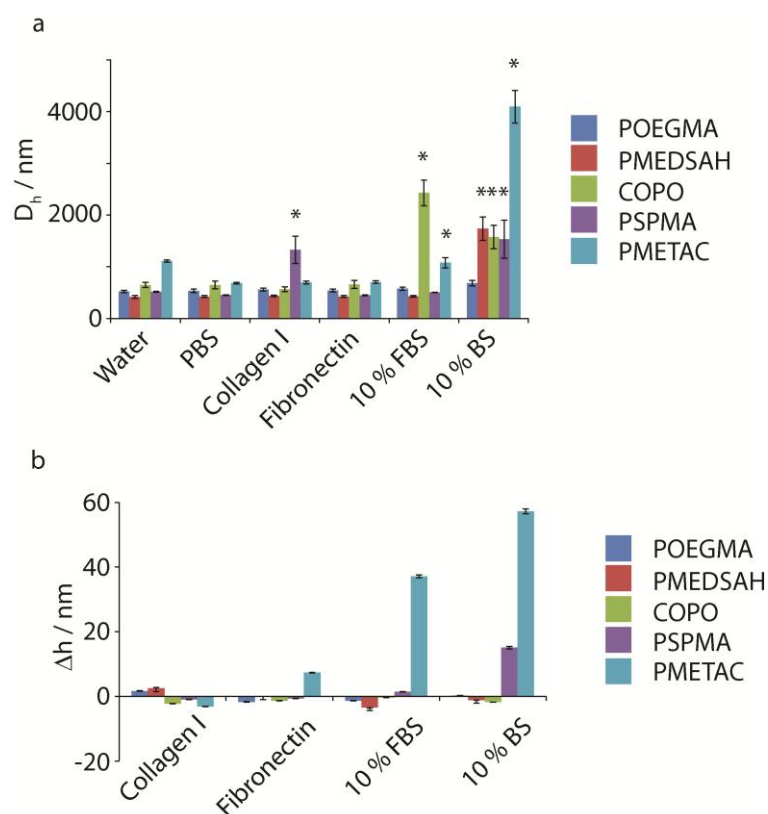


Figure S4. Protein adsorption on polymer brushes. a, Protein adsorption to brush-coated silica particles (320 nm) was followed by particle sizing (DLS). Asterisks (*) denote apparent particle aggregation and sedimentation over extended periods of time. b, Change in dry ellipsometric thickness following exposure of brushes to protein solutions.

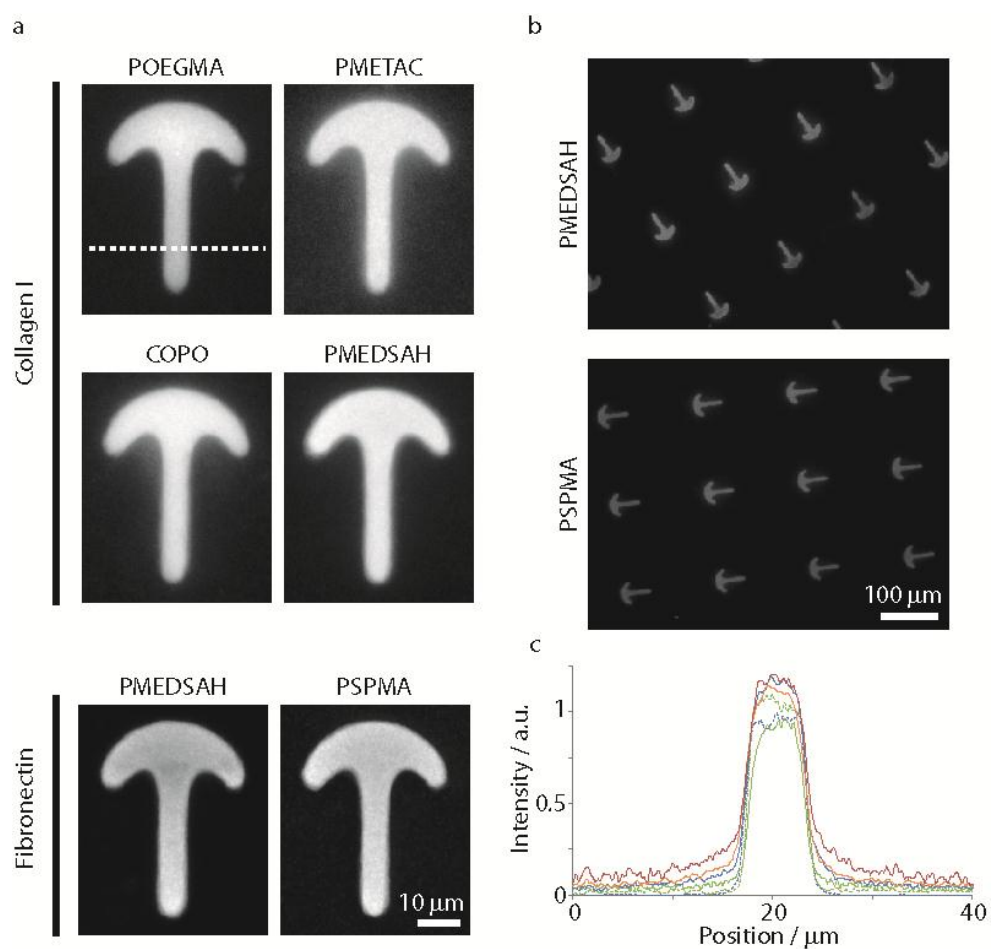


Figure S5. ECM protein patterns using polymer brushes. a, Overlay of single collagen type I and fibronectin patterns (arc-shaped) deposited on polymer brushes and visualised using immunofluorescence staining. b, examples of fibronectin patterns obtained using PMEDSAH and PSPMA brushes. c, Profiles of fluorescence intensity across pattern overlays (following dotted line in S5a; POEGMA/Col, green; PMEDSAH/Col, blue; PMEDSAH/Fn, blue dotted; COPO/Col, orange; PMETAC/Col, red; PSPMA/Fn, green dotted).

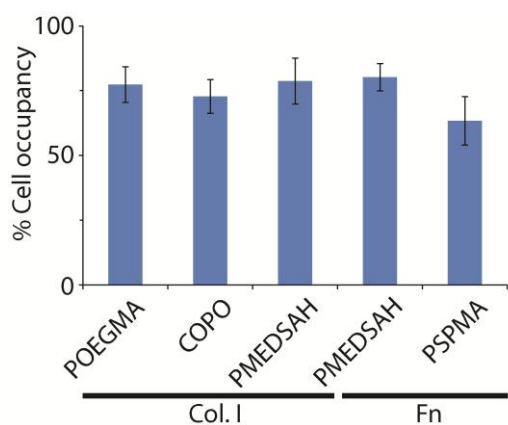


Figure S6. Quantification of cell occupancy. Cell micro-patterns (20 μm) generated for live/dead assay were analysed to quantify the level of occupancy. Cell patterns in which all positions of the brush template are filled would result in 100 % occupancy.

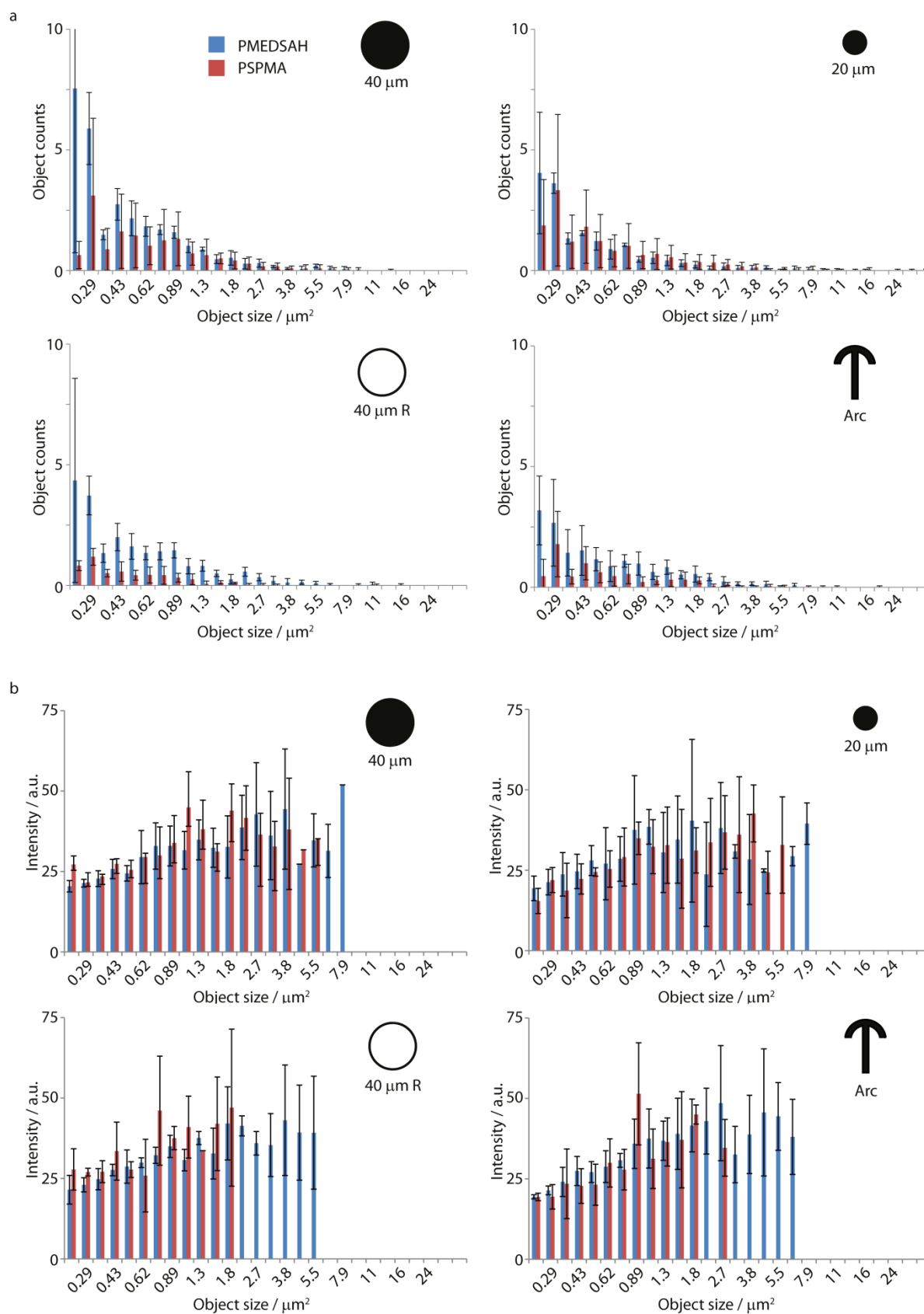


Figure S7. Impact of pattern geometry and brush charge density on focal adhesion distribution. a, Focal adhesion distributions obtained from single cell vinculin stainings (Biological triplicate, $n > 15$ cells in each replicate). b, Associated distribution of vinculin intensities.